A New Tuning Method of Multi-Resonant Current Controllers for Grid-Connected Voltage Source Converters

Xie, Chuan; Zhao, Xin; Li, Kai; Zou, Jianxiao; Guerrero, Josep M.

Published in:
IEEE Journal of Emerging and Selected Topics in Power Electronics

DOI (link to publication from Publisher):
10.1109/JESTPE.2018.2833806

Publication date:
2019

Document Version
Accepted author manuscript, peer reviewed version

A New Tuning Method of Multi-Resonant Current Controllers for Grid-Connected Voltage Source Converters

Chuan Xie, *Member, IEEE,* Xin Zhao, *Student Member, IEEE,* Kai Li, *Member, IEEE,* Jianxiao Zou, Josep M. Guerrero, *Fellow, IEEE*

***Abstract*—Resonant controllers (RSCs) are widely adopted for controlling power converters since they can track AC signals of both positive and negative sequences without steady-state error. However, the performance of RSCs has not been fully exploited due to the improper phase compensation angle and insufficient controller gain. In this paper, a novel controller parameters design method, which is based on the system error transfer function, is proposed to further explore the potential high performance of RSCs. Comparing with the conventional methods, more appropriate phase compensation angles can be obtained, which means that the stable region of the controller gain is extended. Since the proposed RSCs design method is able to maximize the controller gain, the controller sensitivity to system frequency variations can be decreased and the system response speed can be improved. The RSCs tuning procedure is given in detail, and comparative experiments between the proposed method and the conventional method are performed to validate the superiority of the proposed method.**

***Index Terms*—Current control, resonant controller, phase compensation, frequency sensitivity, voltage source converters (VSC).**

I. Introduction

GRID-CONNECTED converters are becoming more and more popular nowadays due to the increasing role of renewable sources and distributed power generation systems [1]–[4]. The voltage source converter (VSC) is one of the most common adopted power electronic interfaces between distributed generation systems and the power grid. One of the most critical control issues for the VSC is how to track the converter current reference in a fast and accurate way. Resonant controllers (RSCs) have been demonstrated to be one of the most suitable candidates and have drawn much research attentions [5]–[15].

The phase lag is one of the vital factors affecting the performance of RSC. One-step and two-step predictions are proposed in [5] to compensate the computational delay, and the harmonic control bandwidth has been extended compared with that of conventional ones without the delay compensation. However, the improvement is limited since the phase lag of the control plant has not been taken into consideration in the delay compensation. The vector proportional-integral (VPI) controller is proposed in [6] to compensate the phase lag of the control plant further, and the harmonic control ability was able to be extended up to the 39th order harmonic. However, the VPI is designed based on the model of the *L*-type filter, and it may not be so perfect for the commonly adopted *LCL*-filter. An arbitrary phase angle compensation strategy for the RSC is proposed in [9], and an equivalent VPI controller on the basis of the phase compensated RSC is investigated in [7]. More appropriate phase compensation angles with improved performance are designed in [10] by maximizing the distance between the Nyquist trajectory to the critical point (minimization of the system sensitivity function). However, it has drawbacks of high calculation complexity and also is not accurate for the *LCL*-filter. Comparing with the method proposed in [10], both the VPI and the method in [7] have relative over-designed phase compensation angle in the low-frequency range and the VPI method also suffers from insufficient phase compensation in the high-frequency range, thus resulting in imperfect performance. In this paper, a more general and simpler tuning method on the phase compensation angle is proposed.

The gain of the RSC is another important aspect that affecting the system performance. The gains of RSCs tuned at different frequencies are usually set to be identical for the sake of simplicity [6], [12], [16], while sometimes they are set to be proportional to the magnitude of the corresponding harmonics to be controlled for achieving a faster response speed [17]. However, how to design the RSC gain to improve the performance is seldom discussed. A methodology that based on the inspection of the pole-zero map of the error closed-loop transfer function is proposed in [11] to assess and optimize the transient response of RSC. However, the locations of dominant

Manuscript received October 19, 2017; revised March 19, 2018; accepted May 2, 2018. Date of publication XXXXX, 2018; date of current version XXXXX, 2018. This work was supported in part by the National Natural Science Foundation of China (No.51707030), the Sichuan Science and technology support program (No. 2016GZ0027&2017GZ0051) and the Fundamental Research Funds for the Central Universities of China (No. ZYGX2015J075).

C. Xie, K. Li and J. Zou are with the School of Automation Engineering, University of Electronic Science and Technology of China, Chengdu 611731, China (e-mail: {c.xie, jxzou}@uestc.edu.cn; autolikai@gmail.com)

X. Zhao is with the School of Automation, Northwestern Polytechnical University, Xi'an 710072, China (e-mail: xzh@nwpu.edu.cn).

J. M. Guerrero is with the Department of Energy Technology, Aalborg University, Aalborg 9220, Denmark (e-mail: joz@et.aau.dk).

This article has been accepted for publication in a future issue of this journal, but has not been fully edited. Content may change prior to final publication. Citation information: DOI 10.1109/JESTPE.2018.2833806, IEEE Journal of Emerging and Selected Topics in Power Electronics

poles will vary with the changing of RSC gain and is designed by trial and error. An analytic design method of the proportional-resonant (PR) controller to achieve the desired transient performance is proposed in [14]. However, the crossover frequency of current loop with PR controller and transient processes time constant is shown to be nonlinearly related, which makes it impossible to design the transient behavior accurately. Meanwhile, the method is based on an ideal *s*-domain model, and the computational and pulse width modulation (PWM) delays are not considered. Besides, the design of RSCs also can be accomplished by formulating a convex optimization problem in terms of linear matrix inequality (LMI) constraints[18] or synthesizing the RSCs within the frame of the linear quadratic regulator (LQR)[19], [20]. These methods are usually time-consuming since many auxiliary states are added to the system, and guess-and-check should be conducted. In this paper, a novel method based on the root locus of the error closed-loop transfer function is proposed to optimize the gains of the RSCs simply.

The paper is organized as follows. Section II reviews the basic concepts of the current control loop and synthesizes the RSCs-based current control loop. The proposed RSCs design method is demonstrated in detail through a step by step design case in Section III, and the designed results are also compared with the ones tuned via previous three different methods in this Section. Experimental results are provided in Section IV to verify the theoretical expectations. Finally, Section V summarizes the paper.

II. Synthesis of the RSCs-based Current Control Loop

Since the RSCs are commonly implemented in a digital manner, all analysis and discussions about the controller design hereinafter will be directly given in z-domain for the sake of the conciseness and high accuracy.

A. Basic Concepts of the Current Control Loop

Fig. 1 shows a modeling of a typical digital current control loop for the grid-connected VSC system[11], [21]. The different signals and blocks are detailed in the following:

1) i is the actual value of output the current;
2) i_{ref} is the current reference; 3) $e = i_{ref} - i$ is the Error;
4) C(z) represents a z-domain current controller;
5) z^{-1} models the computational delay;
6) a zero-order hold (ZOH) is used to model the pulse width modulation (PWM) process (therefore, the total delay time taken into consideration in this paper is one and a half sampling period, which is commonly adopted for the digital control of power inverters [21]).

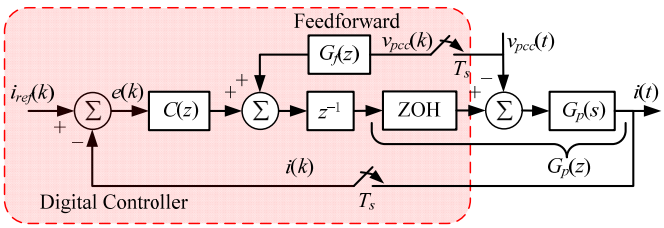

Fig. 1. Block diagram of a typical digital current control loop.

7) G_p(s) is the s-domain plant transfer function of the interface filter. For fair comparison reason, a first-order L-type filter is adopted in this paper the same as used in the literatures [6], [7], [10]. G_p(s) can be expressed as

$$G_p(s) = \frac{1}{L_f s + R_f}. \tag{1}$$

where R_f and L_f are the resistance and inductance of the L-type filter, respectively.

8) v_{pcc} is the voltage of the point of common coupling (PCC), which is fed forward to improve the system transient response under the presence of grid voltage disturbance.

9) G_f(z) represents a filter used to further improve the performance of the voltage feedforward[22]. In this paper, it has been treated as 1 for the sake of simplification.

Applying the ZOH transformation to G_p(s), the corresp -onding z-domain plant transfer function can be derived as [7]

$$G_p(z) = \frac{1}{R_f}\frac{1-e^{R_f T_s / L_f}}{z-e^{R_f T_s / L_f}}. \tag{2}$$

where T_s is the sampling/control period.

B. Synthesis of the RSCs-based Current Controller

As well know, the RSC has an infinite gain at the resonant frequency, which ensure perfect steady-state tracking and disturbance rejection for components pulsating at the resonant frequency when implemented in the closed-loop. Multiple paralleled RSCs based current controller is highly popular in active power filter applications for harmonic tracking [5]–[7], [23], and in some other applications for better rejection of harmonics in the PCC [24], [25]. Commonly, the RSCs are paralleled with the proportional (P) controller to construct the proportional-resonant controller or proportional-multi-resonant controller. The current controller C(z) is studied in this paper composed of a proportional (P) controller and multiple RSCs, which can be expressed as

$$C(z) = K_p + \sum_{h \in N_h} G_{rh}(z). \tag{3}$$

where K_p is the proportional gain, $G_{rh}(z)$ is the RSC tuned at h order harmonic, N_h is the set of selected harmonic orders. The z-domain transfer function of phase compensated RSC can be expressed as [26]

$$G_{rh}(z) = K_{Ih}\frac{1}{h\omega_1}\frac{az^2 + bz + c}{z^2 + dz + 1}. \tag{4}$$

where $a = [\sin(h\omega_1 T_s + \varphi_h) - \sin(\varphi_h)] / 2$, $b = [\cos(h\omega_1 T_s) - 1]\sin(\varphi_h)$, $c = [-\sin(h\omega_1 T_s - \varphi_h) - \sin(\varphi_h)] / 2$, $d = -2\cos(h\omega_1 T_s)$, h is harmonic order, ω_1 is the fundamental angular frequency, K_{Ih} is the integral gain and φ_h is the phase compensation angle. Note that the $G_{rh}(z)$ is derived from the corresponding s-domain transfer function via pre-warped Tustin Transformation [26].

C. the Error Closed-loop Transfer Function

Assuming that the feedforward can counteract the disturbance of v_{pcc}, the block diagram of the digital current control loop shown in Fig. 1 can be simplified as z-domain block diagram shown in Fig. 2.

This article has been accepted for publication in a future issue of this journal, but has not been fully edited. Content may change prior to final publication. Citation information: DOI 10.1109/JESTPE.2018.2833806, IEEE Journal of Emerging and Selected Topics in Power Electronics

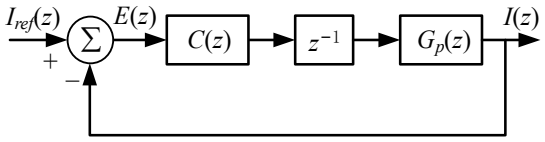

Fig. 2. Block diagram of the current control loop in z-domain.

According to Fig. 2, the error closed-loop transfer functions can be derived as

$$G_e(z)=\frac{E(z)}{I_{ref}(z)}=\frac{1}{1+C(z)z^{-1}G_p(z)}$$
$$=\frac{1}{1+[K_p+\sum_{h\in N_h}G_{rh}(z)]z^{-1}G_p(z)}$$
$$=\frac{\overbrace{\frac{1}{1+K_pz^{-1}G_p(z)}}^{G_{e1}(z)}\cdot\overbrace{\frac{1}{1+\sum_{h\in N_h}G_{rh}(z)G_c(z)/K_p}}^{G_{e2}(z)}}{}. \quad (5)$$

where $G_c(z)=K_pz^{-1}G_p(z)/[1+K_pz^{-1}G_p(z)]$ to represent the closed-loop transfer function with only P control.

From (5), it can be observed that the error is bounded if the following two conditions hold.

i) the roots of $1+K_pz^{-1}G_p(z)=0$ are inside the unit circle,

ii) the roots of $1+\sum_{h\in N_h}G_{rh}(z)G_c(z)/K_p$ are also inside the unit circle.

It can be seen from (5) that $\left|G_{e2}(e^{j\omega T_s})\right|\times\left|G_{e2}(e^{j\omega T_s})\right|$ represents the system steady-state error with only P control, and the system steady-state error becomes $\left|G_{e2}(e^{j\omega T_s})\right|$ times smaller after the RSCs are embedded. Due to the infinite gains of the RSCs at the resonant frequencies, i.e., $\lim_{\omega\to h\omega_1}\sum_{h\in N_h}\left|G_{rh}(e^{j\omega T_s})\right|=\infty$, zero steady-state error can be achieved at the resonant frequencies, i.e., $\lim_{\omega\to h\omega_1}\left|E(e^{j\omega T_s})\right|=\lim_{\omega\to h\omega_1}\left|G_{e2}(e^{j\omega T_s})\right|\times\left|G_{e1}(e^{j\omega T_s})\right|\times\left|I_{ref}(e^{j\omega T_s})\right|=0$.

According to the first stability condition, the root locus of $1+K_pz^{-1}G_p(z)$ can be drawn to tune the value of K_p. And the second stability condition can be inspected by applying Nyquist stability criterion to the open-loop transfer function, i.e., $\sum_{h\in N_h}G_{rh}(z)G_c(z)/K_p$, then the phase compensation angles of the selected RSCs can be determined by maximizing the system stability margin. Besides, the integral gains of the selected RSCs also can be tuned via the root locus of $1+\sum_{h\in N_h}G_{rh}(z)G_c(z)/K_p$.

III. The Proposed Controller Parameters Tuning Method

A three-phase compact islanded microgrid test bed is built in the laboratory, and the corresponding equivalent single-line block diagram is shown in Fig. 3. As can be seen from Fig. 3 that the experimental testbed consists of two converters, one of them serves as grid forming VSC which is connected to the AC bus through an *LCL*-type filter, while the other one acts as grid-connected VSC which is filtered with single-*L* filter and connected to the AC bus through an isolated transformer. The proposed methodology is particularized for the grid-connected VSC with L_f =5 mH, R_f =0.5 Ω. The control frequency is 10 kHz.

A. Tune of the Proportional Gain K_p

To ensure the first stability condition, the root locus of $1+K_pz^{-1}G_p(z)$ is drawn in Fig. 4 to tune the value of K_p. It can be observed from the Fig. 4 that, the upper boundary of K_{pmax} is 50 Ω. Nevertheless, K_p is selected to be 17 Ω to obtain sufficient system damping, i.e., ζ = 0.707, in order to avoid system oscillation.

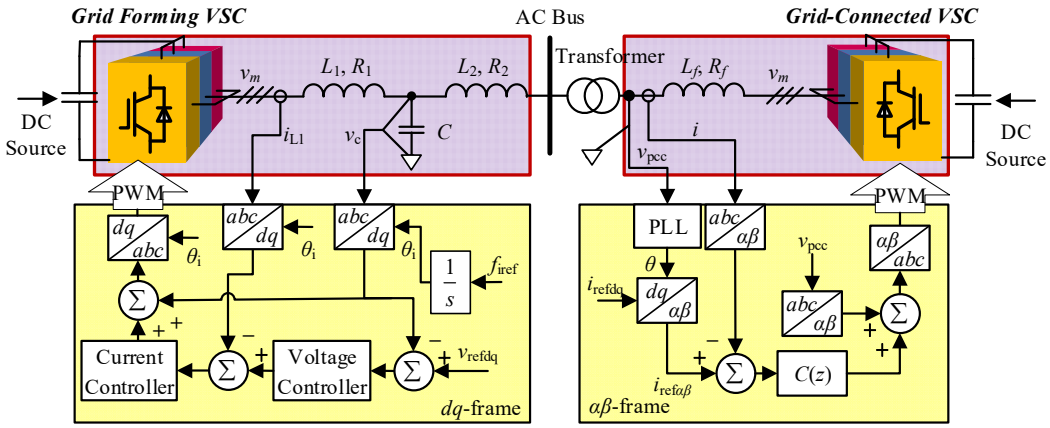

Fig. 3. Equivalent single-line block diagram of the built experimental test bed in the laboratory.

This article has been accepted for publication in a future issue of this journal, but has not been fully edited. Content may change prior to final publication. Citation information: DOI 10.1109/JESTPE.2018.2833806, IEEE Journal of Emerging and Selected Topics in Power Electronics

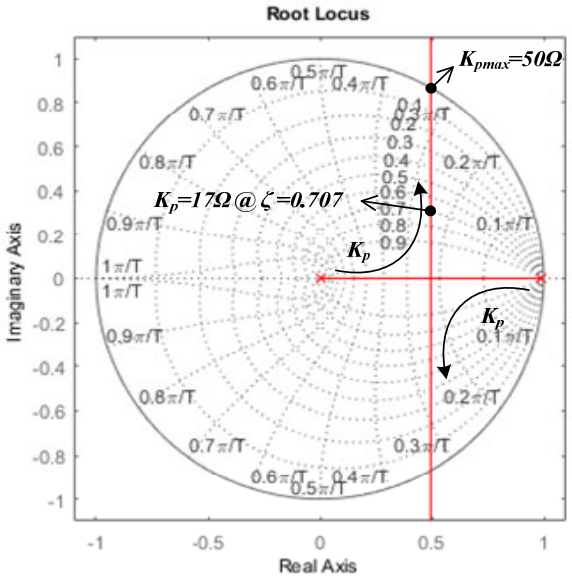

Fig. 4. Root locus of $1+K_p z^{-1}G_p(z)$.

Bode plots of the closed-loop transfer function with only P control, i.e., G_c(z), are presented in Fig. 5, in which it can be observed that the system bandwidth increases as K_p increased, meanwhile, a resonant peak may appear in the system closed-loop magnitude characteristic if K_p is too large. Thus, the proportional gain K_p should be well designed to obtain a large system bandwidth as well as a smooth magnitude characteristic. In this studied case, K_p equals to 17 Ω seems to be a good tradeoff between the bandwidth and the closed-loop magnitude characteristic. Nonetheless, it is worth noting that the system harmonic control capability is limited, due to the large phase lag in high frequencies range, e.g., a 110º phase lag at 1 kHz. Therefore, to enhance the system harmonic control capability, the harmonic compensator regarding dominant harmonic components (5th, 7th, 11th, 13th) are added.

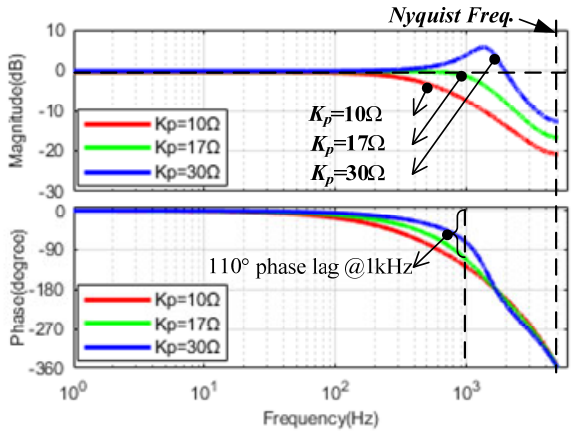

Fig. 5. Bode plots of the closed-loop transfer function with only P control under different proportional gains.

B. Tune of the Phase Compensation Angle φ_h

The second stability condition is inspected by applying Nyquist stability criterion to the open-loop transfer function of $\sum_{h\in N_h} G_{rh}(z)G_c(z)/K_p$. According to the Nyquist stability criterion, the number of the open-loop unstable poles P must equal to N, the net number of counter-clockwise encirclements of the critical point (-1, j0) on the Nyquist diagram, to ensure system stability, i.e., $P = N$ [27]. When $P = 0$, the distance between the Nyquist curve and the critical point (-1, j0) can provide a clear indication of stability margin [10]. To achieve sufficient stability margin, the phase compensation angle is set equal to the phase lag of G_c(z), i.e.

$$\varphi_h = -\angle G_c(e^{jh\omega_1 T_s}) \tag{6}$$

To show the superiority of this design criterion intuitively, the Nyquist diagrams of $\sum_{h\in N_h} G_{rh}(z)G_c(z)/K_p$ with RSC tuned at the fundamental frequency under different compensation angles shown in Fig. 6 as an example. It can be seen that the system stability margin is maximized with the proposed phase compensation angle since the distance between the Nyquist trajectory and the critical point (denoted by η_3) is maximized. Note that the phase compensation angle tuned via VPI method in [6] is obviously over-designed compensated, the distance between the Nyquist trajectory and the critical point (denoted by η_2) is not increased but decreased when compared with the conventional one with no phase compensation (denoted by η_1).

The phase compensation angles calculated via different methods [6], [7], [10] are plotted in Fig. 7 for the sake of intuitive comparison. It can be observed from Fig. 7 that, compared with the phase compensation angle tuned via the proposed method, the one obtained with the methods in [6], [7] and [6], [7] are over-designed compensated in the low-frequency range, and the VPI also suffers from the insufficient phase compensation in the high-frequency range. This conclusion can be further

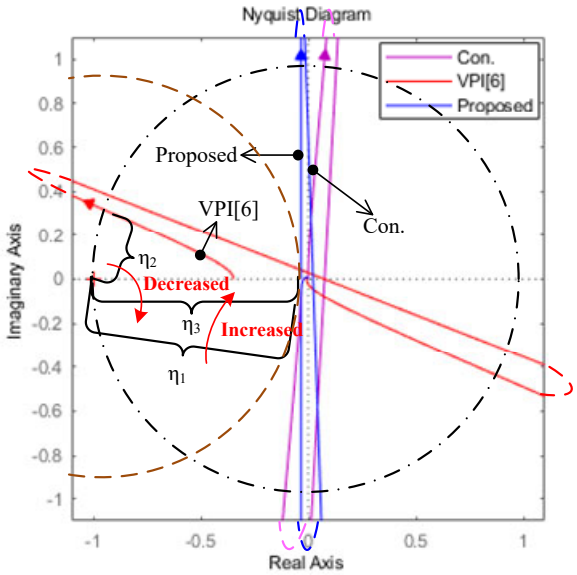

Fig. 6. Nyquist diagrams of $\sum_{h\in N_h} G_{rh}(z)G_c(z)/K_p$ with RSC tuned at the fundamental frequency under different compensation angles.

This article has been accepted for publication in a future issue of this journal, but has not been fully edited. Content may change prior to final publication. Citation information: DOI 10.1109/JESTPE.2018.2833806, IEEE Journal of Emerging and Selected Topics in Power Electronics

confirmed in Section II.C. Note that the phase compensation angle tuned via the proposed method is similar to the one obtained in [10] by minimizing sensitivity function. However, the method in [10] seems to be a bit complex for the first-order *L*-type filter, let alone when it's applied to the high-order filters, e.g., *LCL*-type filter. By contrast, the effectiveness of the proposed design method does not rely on the specific type of interface filter, the transfer function of the *L*-type filter, i.e., Eq. (1), can be replaced by that of the *LCL*-type filter, and thus theproposed method can be easily extended to the *LCL*-filtered VSC application. In addition, the tuned phase compensation angles of selected RSCs via different methods are also listed in TABLE I for further controller parameters design.

C. Tune of the RSCs Gains

The integral gains of RSCs are also constrained by the second stability condition, the root locus of $1+\sum_{h\in N_h} G_{rh}(z)G_c(z)/K_p$ is drawn to check the upper boundaries of the integral gains. For the sake of simplicity, the gains of the selected RSCs are set to be identical to each other. The root locus of $1+\sum_{h\in N_h} G_{rh}(z)G_c(z)/K_p$ with phase compensation angles tuned via VPI is plotted in Fig. 8 as an example, the upper boundary of K_{Ih} is 3472 $\Omega\cdot s^{-1}$. The upper boundaries of the integral gains for RSCs with different phase compensation angles are obtained via the same method and compared in TABLE II. It can be observed from TABLE II that the higher upper boundary can be obtained with the phase compensation angles tuned via the proposed method and the one in [10], which implies faster response speed and better frequency adaptivity due to the potential increased integral gain. It also confirms the superiority of the proposed method, since that only with more appropriate phase compensation angle a wider system stability region with higher upper boundary can be achieved.

The error convergence speed can be reflected via the step response of (5), which can be easily plotted with Matlab. The settling times of the step response of the error transfer function under different integral gains of RSCs are plotted in Fig. 9. It

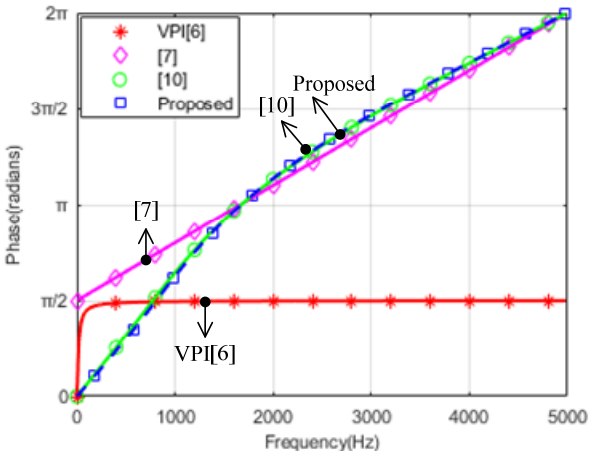

Fig. 7. The phase compensation angles obtained via different methods.

TABLE I. THE TUNED PHASE COMPENSATION ANGLES OF THE SELECTED RSCS VIA DIFFERENT METHODS

Symbol	VPI[6]	[7]	[10]	Proposed
φ_1(rad)	1.26	1.62	0.10	0.09
φ_5(rad)	1.51	1.81	0.49	0.46
φ_7(rad)	1.53	1.90	0.70	0.65
φ_{11}(rad)	1.54	2.09	1.11	1.04
φ_{13}(rad)	1.55	2.18	1.31	1.24

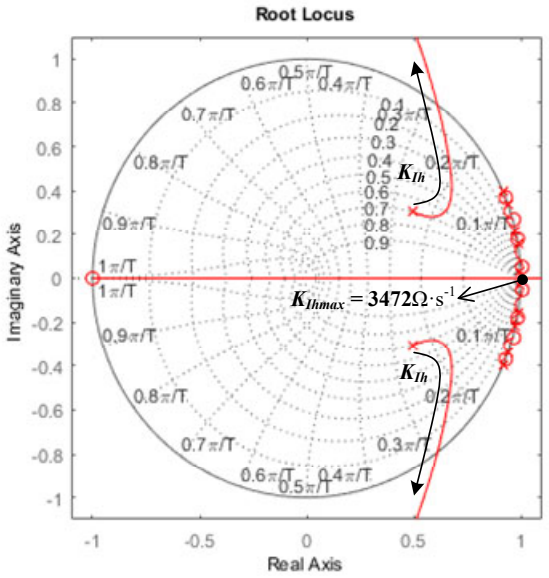

Fig. 8. The root locus of $1+\sum_{h\in N_h} G_{rh}(z)G_c(z)/K_p$ with phase compensation angles tuned via VPI [6].

TABLE II. UPPER BOUNDARIES OF K_{Ih} FOR RSCS WITH DIFFERENT PHASE COMPENSATION ANGLES.

Symbol	VPI [6]	[7]	[10]	Proposed
$K_{Ihmax}(\Omega\cdot s^{-1})$	3472	3455	11536	12176

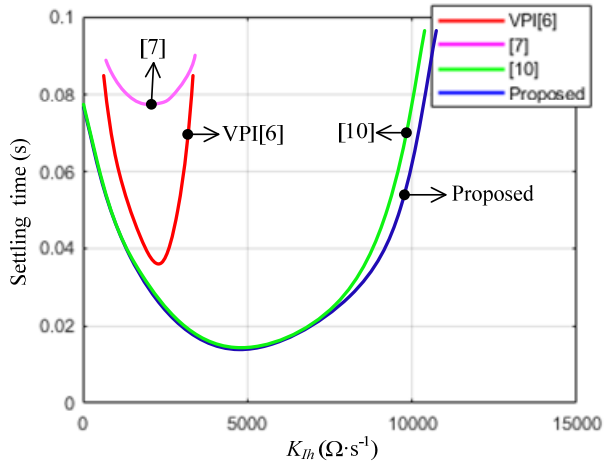

Fig. 9. Settling times of the step response of the error transfer function under different integral gains of RSCs.

can be seen that the larger integral gain does not always mean

This article has been accepted for publication in a future issue of this journal, but has not been fully edited. Content may change prior to final publication. Citation information: DOI 10.1109/JESTPE.2018.2833806, IEEE Journal of Emerging and Selected Topics in Power Electronics

the shorter settling time. Setting K_{Ih} equals to the half of K_{1hmax} is a good tradeoff between the response speed and the frequency adaptivity.

IV. Experimental Verification

Fig. 10 shows the experimental setup, in which two 2.2-kW *Danfoss* inverters are utilized as the grid-forming inverter and the grid following inverter, respectively. The DC link voltage is set to 350 V, the nominal phase voltage and grid frequency are controlled to be 110 V and 50 Hz, respectively. The control algorithm is implemented in dSPACE 1005 system with a 10 kHz sampling/switching frequency. Due to the similarity of the parameters tuned via VPI and the method in [6], [7] as well as the ones tuned via the proposed method and the one in [10] as listed in TABLE I and II, only the parameters tuned via the proposed method and VPI are experimentally compared.

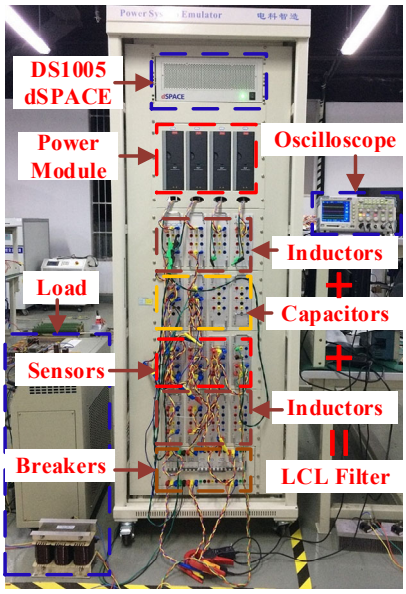

Fig. 10. Hardware setup including the inverters and the control platform.

A. The Steady-State Performance Evaluation

The steady-state performance of the current controller is tested under highly distorted grid voltage containing an amount of 5th, 7th, 11th and 13th order harmonics. The experimental waveforms are given in Fig. 11, in which from up to bottom are grid voltage, current reference and inverter output current, and current tracking error, respectively.

It can be observed from Fig. 11 that the output current is highly distorted with only P control due to the poor harmonic rejection capability. After enabling the RSCs, the dominant current harmonics are attenuated about 20dB as shown in Fig. 12, which validates the high harmonic rejection capability of the RSCs.

B. The Dynamic Performance Evaluation

The dynamic experiments are conducted by stepping the current reference from 0 Ampere to 5 Ampere, and the corresponding results are presented in Figs. 13 and 14. The system response speed is evaluated via the tracking error convergence speed. It can been seen from Figs. 13 and 14 that two things are apparent: 1) too larger integral gain of RSC will slow the response speed; 2) the RSCs tuned via the proposed scheme can achieve faster response speed. The dynamic experimental results agree well with the theoretical expectations. Moreover, it can be observed from Fig. 14(c) that if the integral gain of RSC is set larger than the upper boundary, the system becomes unstable and the inverter is tripped.

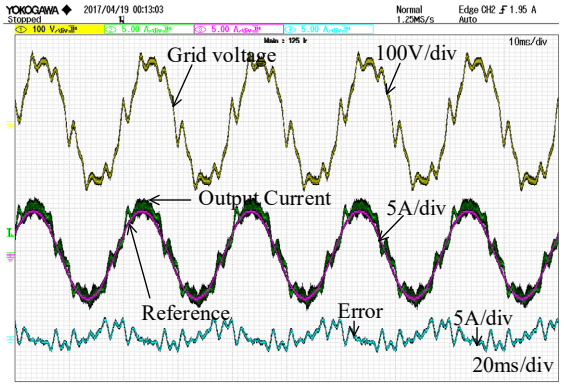

(a)

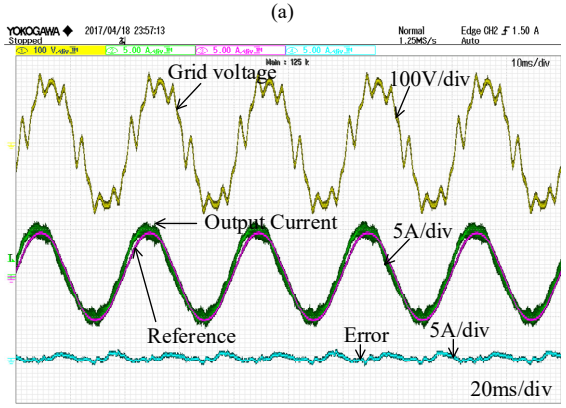

(b)

Fig. 11. Experimental waveforms with (a) P and (b) proposed RSCs under the rated grid frequency.

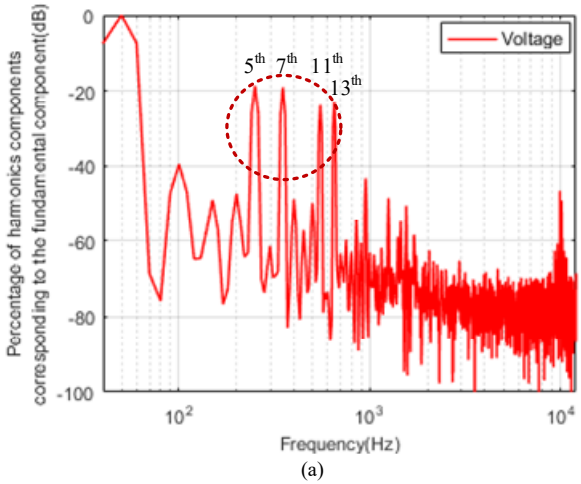

(a)

This article has been accepted for publication in a future issue of this journal, but has not been fully edited. Content may change prior to final publication. Citation information: DOI 10.1109/JESTPE.2018.2833806, IEEE Journal of Emerging and Selected Topics in Power Electronics

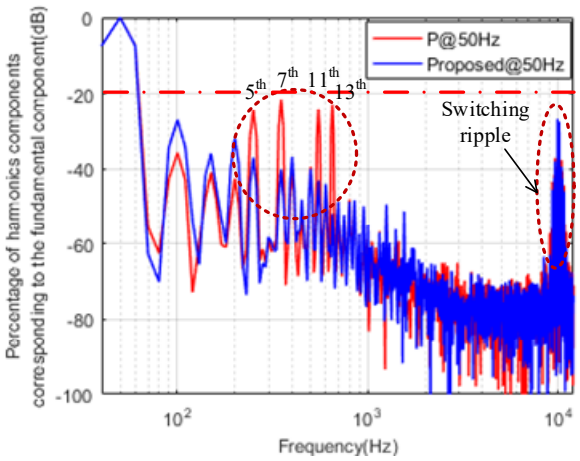

(b)

Fig. 12. Spectra of (a) grid voltage and (b)the inverter output current under the rated grid frequency.

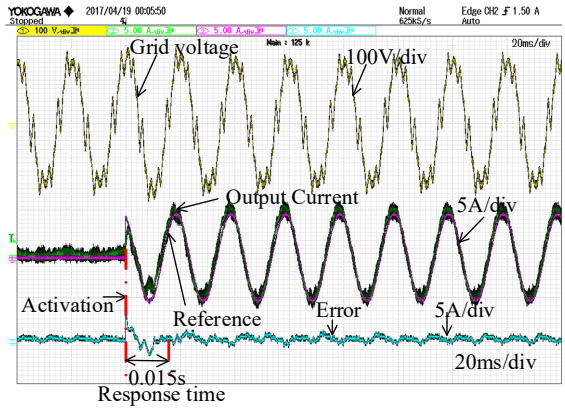

(a)

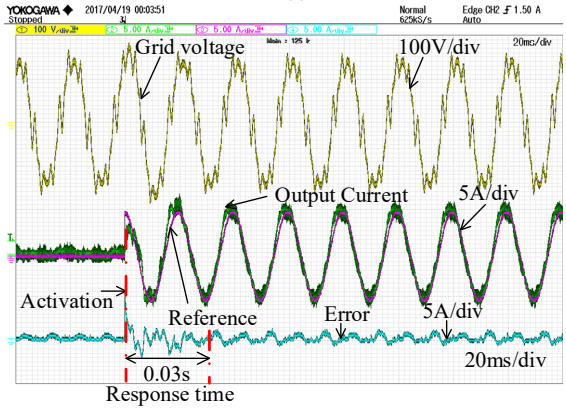

(b)

Fig. 13. Dynamic experimental waveforms with RSCs tuned via proposed scheme. (a) K_{Ih}=6000 Ω·s^{-1}, (b) K_{Ih}=9000 Ω·s^{-1}.

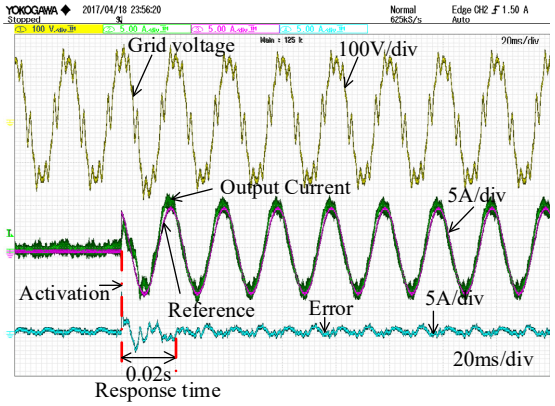

(a)

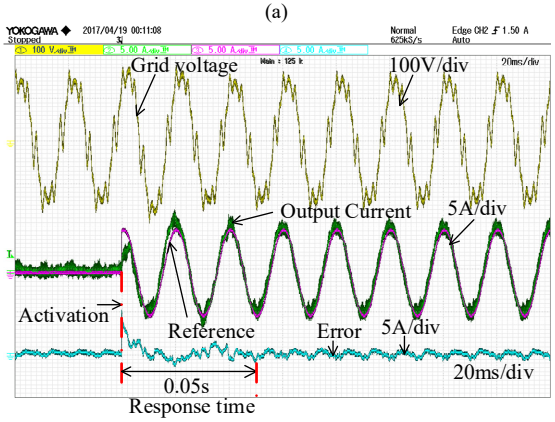

(b)

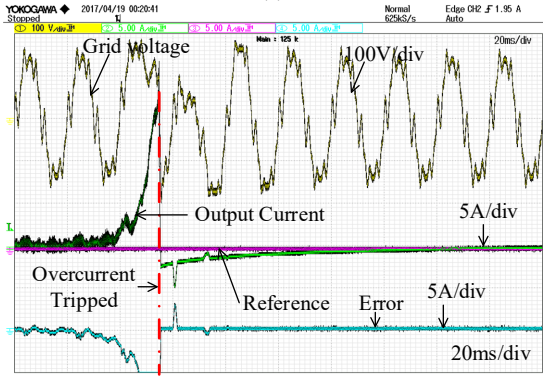

(c)

Fig. 14. Dynamic experimental waveforms with RSCs tuned via VPI. (a) K_{Ih}= 1800Ω·s^{-1}, (b) K_{Ih}= 3000Ω·s^{-1}, (c) K_{Ih}=6000Ω·s^{-1}.

C. *Frequency Adaptivity Performance Evaluation*

Fig. 15 shows the spectra of the inverter output currents under different grid frequencies to evaluate the frequency adaptivity of the RSCs tuned via VPI and the proposed method. From Fig. 15, it can be observed that although the performance of RSCs degrades to some extent in the presence of ±1Hz grid frequency variation, the RSCs tuned via the proposed scheme can achieve better frequency adaptivity than the RSCs tuned via VPI, which also complies well with the theoretical analysis.

This article has been accepted for publication in a future issue of this journal, but has not been fully edited. Content may change prior to final publication. Citation information: DOI 10.1109/JESTPE.2018.2833806, IEEE Journal of Emerging and Selected Topics in Power Electronics

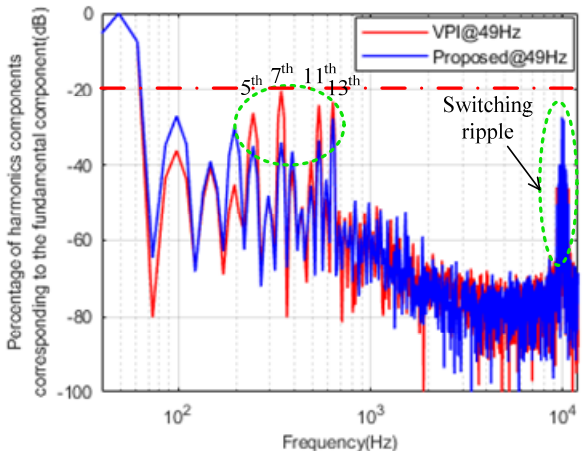

(a)

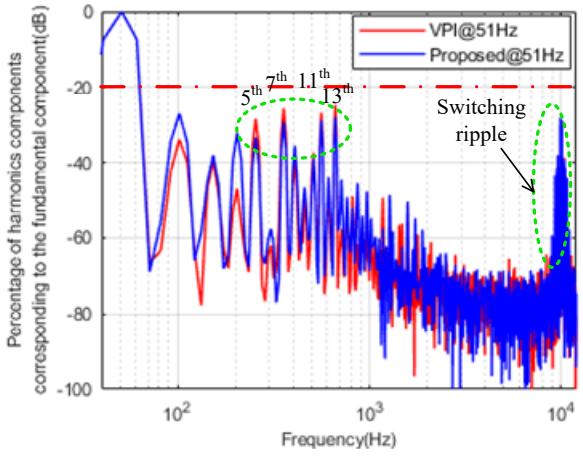

(b)

Fig. 15. Spectra of inverter output currents under different grid frequencies. (a) 49 Hz, (b) 51 Hz.

V. Conclusion

To improve the performance of RSCs-based current controller for the grid-connected VSCs further, a novel controller parameters design method, which is based on the error transfer function, is proposed in this paper. Comparing with the VPI, the proposed method can obtain a more appropriate phase compensation angle, as well as a wider stable region of the controller gain, such that a smaller frequency sensitivity and a faster response speed of RSC are achieved. Moreover, the proposed tuning method is more convenient than the one based on minimization the system sensitivity function. Although the given design case is particularized for the *L*-filtered converter for the sake of fair comparison with existing methods, the effectiveness of the proposed design method is independent of the type of the filter, can be easily extended to the *LCL*-filtered VSC applications.

References

[1] J. M. Guerrero *et al.*, "Distributed Generation: Toward a New Energy Paradigm," *IEEE Ind. Electron. Mag.*, vol. 4, no. 1, pp. 52–64, Mar. 2010.

[2] K. Li, H. Xu, Q. Ma, and J. Zhao, "Hierarchy Control of Power Quality for Wind-Battery Energy Storage System," *IET Power Electron.*, vol. 7, no. 8, pp. 2123–2132, Aug. 2014.

[3] Q. Wang, M. Cheng, Y. Jiang, W. Zuo, and G. Buja, "A Simple Active and Reactive Power Control for Applications of Single-Phase Electric Springs," *IEEE Trans. Ind. Electron.*, vol. 65, no. 8, pp. 6291–6300, Aug. 2018.

[4] K. Li, M. Wei, C. Xie, F. Deng, J. M. Guerrero, and J. C. Vasquez, "Triangle Carrier based Discontinuous PWM for Three-Level NPC Inverters," *IEEE J. Emerg. Sel. Top. Power Electron.*, vol. PP, no. 99, pp. 1–1, 2018.

[5] X. Yuan, W. Merk, H. Stemmler, and J. Allmeling, "Stationary-Frame Generalized Integrators for Current Control of Active Power Filters with Zero Steady-State Error for Current Harmonics of Concern Under Unbalanced and Distorted Operating Conditions," *Ind. Appl. IEEE Trans. On*, vol. 38, no. 2, pp. 523–532, Mar. 2002.

[6] C. Lascu, L. Asiminoaei, I. Boldea, and F. Blaabjerg, "High Performance Current Controller for Selective Harmonic Compensation in Active Power Filters," *IEEE Trans. Power Electron.*, vol. 22, no. 5, pp. 1826–1835, Sep. 2007.

[7] A. G. Yepes, F. D. Freijedo, O. Lopez, and J. Doval-Gandoy, "High-Performance Digital Resonant Controllers Implemented With Two Integrators," *IEEE Trans. Power Electron.*, vol. 26, no. 2, pp. 563–576, Feb. 2011.

[8] C. Attaianese, M. Di Monaco, and G. Tomasso, "High Performance Digital Hysteresis Control for Single Source Cascaded Inverters," *IEEE Trans. Ind. Inform.*, vol. 9, no. 2, pp. 620–629, May 2013.

[9] R. I. Bojoi, G. Griva, V. Bostan, M. Guerriero, F. Farina, and F. Profumo, "Current Control Strategy for Power Conditioners Using Sinusoidal Signal Integrators in Synchronous Reference Frame," *IEEE Trans. Power Electron.*, vol. 20, no. 6, pp. 1402–1412, Nov. 2005.

[10] A. G. Yepes, F. D. Freijedo, O. Lopez, and J. Doval-Gandoy, "Analysis and Design of Resonant Current Controllers for Voltage-Source Converters by Means of Nyquist Diagrams and Sensitivity Function," *IEEE Trans. Ind. Electron.*, vol. 58, no. 11, pp. 5231–5250, Nov. 2011.

[11] A. Vidal *et al.*, "Assessment and Optimization of the Transient Response of Proportional-Resonant Current Controllers for Distributed Power Generation Systems," *IEEE Trans. Ind. Electron.*, vol. 60, no. 4, pp. 1367–1383, Apr. 2013.

[12] S. Golestan, E. Ebrahimzadeh, J. M. Guerrero, and J. Vasquez, "An Adaptive Resonant Regulator for Single-Phase Grid-Tied VSCs," *IEEE Trans. Power Electron.*, vol. PP, no. 99, pp. 1–1, 2017.

[13] H. Yi, F. Zhuo, and F. Wang, "Analysis About Overshoot Peaks Appearing in the Current Loop With Resonant Controller," *IEEE J. Emerg. Sel. Top. Power Electron.*, vol. 4, no. 1, pp. 26–36, Mar. 2016.

[14] A. Kuperman, "Proportional-Resonant Current Controllers Design Based on Desired Transient Performance," *IEEE Trans. Power Electron.*, vol. 30, no. 10, pp. 5341–5345, Oct. 2015.

[15] C. Xie, X. Zhao, K. Li, D. Liu, J. M. Guerrero, and J. C. Vasquez, "Phase Compensated Reduced Order Generalized Integrators for Grid-Tied VSCs with Harmonics Compensation Capability," *IEEE Trans. Ind. Appl.*, vol. 54, no. 3, pp. 1–11, 2018. 10.1109/TIA.2018.2816900

[16] L. Harnefors, A. G. Yepes, A. Vidal, and J. Doval-Gandoy, "Passivity-Based Stabilization of Resonant Current Controllers With Consideration of Time Delay," *IEEE Trans. Power Electron.*, vol. 29, no. 12, pp. 6260–6263, Dec. 2014.

[17] Y. Yang, K. Zhou, M. Cheng, and B. Zhang, "Phase Compensation Multiresonant Control of CVCF PWM Converters," *IEEE Trans. Power Electron.*, vol. 28, no. 8, pp. 3923–3930, Aug. 2013.

[18] L. F. A. Pereira, J. V. Flores, G. Bonan, D. F. Coutinho, and J. M. G. da Silva, "Multiple Resonant Controllers for Uninterruptible Power Supplies-A Systematic Robust Control Design Approach," *IEEE Trans. Ind. Electron.*, vol. 61, no. 3, pp. 1528–1538, Mar. 2014.

[19] A. Hasanzadeh, C. S. Edrington, B. Maghsoudlou, F. Fleming, and H. Mokhtari, "Multi-Loop Linear Resonant Voltage Source Inverter Controller Design for Distorted Loads Using the Linear Quadratic Regulator Method," *IET Power Electron.*, vol. 5, no. 6, pp. 841–851, Jul. 2012.

[20] B. Ufnalski, A. Kaszewski, and L. M. Grzesiak, "Particle Swarm Optimization of the Multioscillatory LQR for a Three-Phase Four-Wire Voltage-Source Inverter With an LC Output Filter," *IEEE Trans. Ind. Electron.*, vol. 62, no. 1, pp. 484–493, Jan. 2015.

[21] S. Buso and P. Mattavelli, *Digital Control in Power Electronics*, First Edition. Morgan&Claypool, 2006.

[22] J. Xu, S. Xie, Q. Qian, and B. Zhang, "Adaptive Feedforward Algorithm Without Grid Impedance Estimation for Inverters to Suppress Grid

Current Instabilities and Harmonics Due to Grid Impedance and Grid Voltage Distortion," *IEEE Trans. Ind. Electron.*, vol. 64, no. 9, pp. 7574–7586, Sep. 2017.

[23] S. Fukuda and T. Yoda, "A Novel Current-Tracking Method for Active Filters Based on a Sinusoidal Internal Model," *Ind. Appl. IEEE Trans. On*, vol. 37, no. 3, pp. 888–895, May 2001.

[24] M. Liserre, R. Teodorescu, and F. Blaabjerg, "Stability of Photovoltaic and Wind Turbine Grid-Connected Inverters for A Large Set of Grid Impedance Values," *IEEE Trans. Power Electron.*, vol. 21, no. 1, pp. 263–272, Jan. 2006.

[25] R. A. Mastromauro, M. Liserre, and A. D. Aquila, "Study of the Effects of Inductor Nonlinear Behavior on the Performance of Current Controllers for Single-Phase PV Grid Converters," *IEEE Trans. Ind. Electron.*, vol. 55, no. 5, pp. 2043–2052, May 2008.

[26] R. Teodorescu, F. Blaabjerg, M. Liserre, and P. C. Loh, "Proportional-Resonant Controllers and Filters for Grid-Connected Voltage-Source Converters," *Electr. Power Appl. IEE Proc.*, vol. 153, no. 5, pp. 750–762, Sep. 2006.

[27] Gene F. Franklin, J. David Powell, and Michael Workman, *Digital Control of Dynamic Systems*, Third Edition. Addison Wesley Longman, 1998.

Chuan Xie (M'16) **received** the B.S. degree in automation engineering from the University of Electronic Science and Technology of China, Chengdu, China, and the Ph.D. degree in power electronics from Zhejiang University, Hangzhou, China, in 2007 and 2012, respectively.

Since 2012, he was a lecturer with the School of Automation Engineering at University of Electronic Science and Technology of China. From May 2015 to May 2016, he was a Visiting Scholar at the Department of Energy Technology, Aalborg University. His main research interests include digital control of power electronics, grid synchronization technology, distributed generation systems, microgrids and power quality.

Xin Zhao (S'15) received the B.S. and M.S. degrees in Power Electronics & Electrical Drives from Northwestern Polytechnical University, Xi'an, China, in 2010 and 2013, respectively, and the Ph.D. degree in electrical engineering from Aalborg University, Denmark, in 2017.

Since 2017, he has been with Northwestern Polytechnical University, Xi'an, China, as an Associate Professor. His research interests include power quality, distributed generation systems, and power electronic converter design, analysis and control.

Kai Li (M'15) received the B.S., M.S., and Ph.D. in Automation Engineering from the University of Electronic Science and Technology of China, Chengdu, China in 2006, 2009, and 2014, respectively.

From 2009 to 2016, he was an Assistant Professor with the School of Automation Engineering, University of Electronic Science and Technology of China, Chengdu, China. From 2016.2 to 2017.2, he was an Guest Researcher with the Department of Energy Technology, Aalborg University, Denmark. Since 2016, he has been an Associate Professor with the School of Automation Engineering, University of Electronic Science and Technology of China, Chengdu, China. His research interests include multilevel inverters, storage converters, and microgrids.

Jianxiao Zou received the B.S., M.S., and Ph.D. degrees in control science and engineering from the University of Electronic Science and Technology of China, Chengdu, China in 2000, 2003, and 2009, respectively.

He is currently a professor at University of Electronic Science and Technology of China (UESTC). He served as Vice Dean of School of Automation Engineering from 2011. He also served as the vice president of Sichuan Electrotechnical Society, vice president of Society for electrical engineering, and the Chairman of member development, Chengdu Section of IEEE China. He was a visiting scholar of University of California, Berkeley (UC Berkeley) in 2010 and senior visiting professor of Rutgers, The State University of New Jersey in 2014. He organized more than 10 international conferences/symposiums as general/program chairs and Session Chair. He has been publishing more than 50 journal papers and has been authorized more than 120 national invention patents. His research interests include control theory and control engineering, renewable energy control technologies, intelligent information processing and control.

Josep M. Guerrero (S'01-M'04-SM'08 -F'15) received the B.S. degree in telecommunications engineering, the M.S. degree in electronics engineering, and the Ph.D. degree in power electronics from the Technical University of Catalonia, Barcelona, in 1997, 2000 and 2003, respectively. Since 2011, he has been a Full Professor with the Department of Energy Technology, Aalborg University, Denmark, where he is responsible for the Microgrid Research Program. From 2012 he is a guest Professor at the Chinese Academy of Science and the Nanjing University of Aeronautics and Astronautics; from 2014 he is chair Professor in Shandong University; and from 2015 he is a distinguished guest Professor in Hunan University.

His research interests is oriented to different microgrid aspects, including power electronics, distributed energy-storage systems, hierarchical and cooperative control, energy management systems, and optimization of microgrids and islanded minigrids.